Chapter 1

Basics of Magnetic Resonance Imaging

MRI has been very successful for imaging parts of the body that are stationary. The major strength of MRI is soft tissue contrast, as illustrated in Fig. 1.1. The major drawback of MRI has been imaging speed. The images in Fig. 1.1 require several minutes to acquire. Many of the new applications of MRI require much faster imaging. Two of these are shown in Fig. 1.2. Figure 1.2a was acquired and reconstructed in real-time at a rate of 10 images per second.

One of the key difficulties with high-speed imaging methods is image reconstruction. The examples in Fig. 1.1 are reconstructed by simply performing a 2D inverse Fast Fourier Transform. The images of Fig. 1.2 require a much more sophisticated reconstruction. These reconstruction methods are the subject of this course.

Figure 1.1: Brain images of a normal volunteer show excellent soft tissue contrast. Figures (a) and (b) are axial images with two different image contrasts. Figure (c) shows the flexibility to image any slice orientation. These images required several minutes to acquire.

1.1 Basics of MRI

While we are primarily concerned with the reconstruction aspects of MRI, we still require a basic understanding of how MRI works. Very complete descriptions of MRI are provided in [1–4]. Here we simply outline the basic elements.

The magnezation that we will ultimately use for imaging is formed by placing the subject in a very strong, very homogeneous magnetic field, as shown in Fig. 1.3. T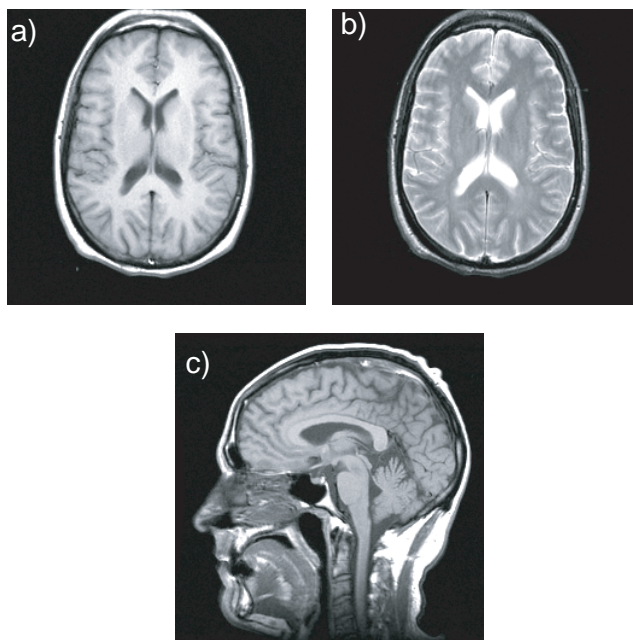his is the polarizing field, denoted B_0. At thermal equalibrium at 1.5T, a few parts per million of the spins, typically protons, in the subject align preferentially in the direction of the field. This population difference is the magnetization that we will use for imaging.

The magnetization interacts with radio frequency energy at its characteristic Larmor frequency

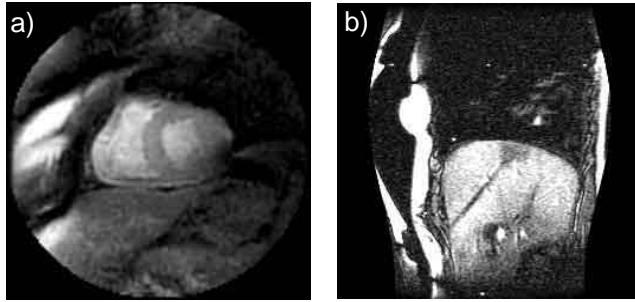$$\omega_0 = \gamma B_0 \quad \text{rad/s} \qquad (1.1)$$

Figure 1.2: New application of MRI, such as real-time imaging of the heart at 10 images per second (a) and the interactive guidance of interventional procedures (b) require high-speed imaging methods, and more sophisticated reconstruction techniques.

or

$$f_0 = \frac{\gamma}{2\pi} B_0 \ \ \text{Hz} \qquad (1.2)$$

where γ is the gyromagnetic ratio, $2\pi \times 4257$ rad/G. Note that for most spins of interest, such as protons, the precession direction is negative. If we apply a short RF pulse, we can tip the magnetization away from the $+z$ axis that is defined by the direction of B_0. MRI is inherently spatially non-selective. If we apply an RF pulse to a volume, all the are spins are tipped, or excited. Unfortunately, performing the spatial encoding for an entire volume is time consuming. Most MRI imaging uses the idea of slice selection to image only a slice through a subject. This is illustrated in Fig. 1.4.
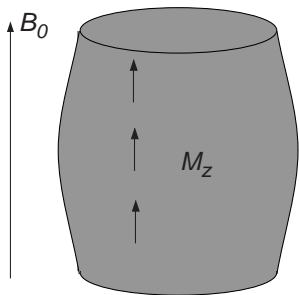

Figure 1.3: An object placed in a strong B_0 field produces a net magnetization along the direction of the polarizing field.
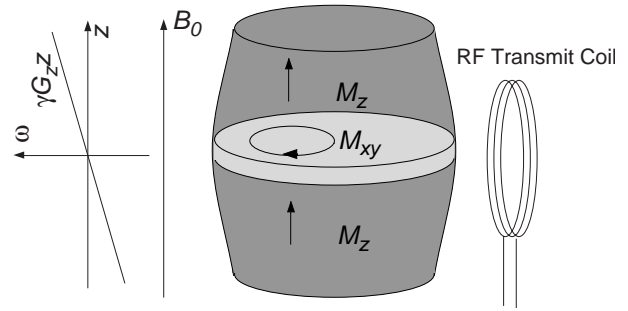

Figure 1.4: A magnetic field with a gradient in the z direction establishes a linear relationship between position and resonant frequency. When the sample is irradiated with an RF pulse at the Larmor frequency γB_0, only the spins at $z = 0$ are on resonance, and are tipped into the transverse plane. Hence, only a slice is excited.

The key idea for slice selection, and all of MRI for that matter, is the use of a small additional field with a $+z$ component that varies linearly in strength with position. This is known as a gradient field. This means that the Larmor frequency now also varies linearly with position,

$$\omega(z) = \gamma G_z z, \qquad (1.3)$$

where G_z is the gradient field strength in G/cm. We then irradiate the subject with an RF pulse with a narrow frequency band. Most spins in the volume will be above or below resonance, and are unaffected. Only the spins whose resonant frequencies are in the RF pulse frequency band will be excited. This excites signal in a a thin slab of material perpendicular to the direction of the gradient field. Gradient fields are available along all three orthogonal axis, and can be combined as a vector to produce a gradient in any desired direction. Hence, any plane orientation can be achieved. The plane is offset in position by choosing the proper band of RF frequencies.

Once a slice has been excited, spins precess around B_0 at $\omega_0 = \gamma B_0$. The spins are then resolved in the remaining two directions by again using linear gradient fields to change the resonant frequencies of spins at different spatial locations. Conceptually, if we apply a gradient in the $+x$ direction (a field

whose $+z$ component varies linearly in proportion to x position), all spins at the same x position will precess at the same frequency. If we acquire the signal produced by the subject, and compute its spectrum, each frequency bin will be proportional to how much magnetization was at that position. Since this is integrated across all spins in the y dimension that have the same x position, what we get is a projection of the object looking in the y dimension. We can then change the direction of the gradient, collect additional projections, and ultimately use projection-reconstruction to reconstruct the slice, just as in X-ray computed tomography [5–6]. This was how MRI was first proposed [7].

In practice. MRI is much more flexible than this, and there are many more desirable acquisition methods. To see how these arise, we first need to more accurately describe the nature of the received signal in MRI.
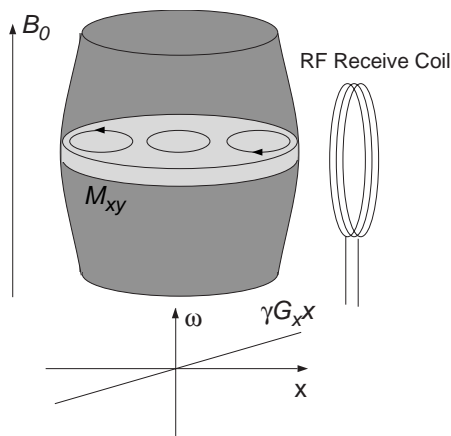

Figure 1.5: A magnetic field with a gradient in the x direction again establishes a linear relationship between position and resonant frequency. Spins at different x positions precess at different frequencies.

1.2 Simple Signal Equation

The goal in MRI is to image the spatial distribution of the transverse magnetization of some object. We will be denoted $M_{xy}(\mathbf{x})$ where the $\mathbf{x}$ is either a two-dimensional vector for slice-selective imaging, or a three-dimensional vector for volumetric imaging. After the transverse magnetization is produced, it precesses at a rate proportional to the local magnetic field. This consists of a large constant bias term B_0, time-invariant local variations in this field $\omega(\mathbf{x})$, and the gradient fields used for imaging $\mathbf{G}(t)$.

The constant term B_0 provides the carrier frequency for the acquisition, but will be ignored here. The $\omega(\mathbf{x})$ term includes the inhomogeneity of the B_0 field, as well as spatial field variations produced by the spatially varying susceptibility of the subject. This will be a major concern, but will also be neglected for the time being. The gradient fields are time-varying magnetic fields that are designed so that the component directed along B_0 is linearly proportional to position.

The precession frequency, which is proportional to the field, is also linearly proportional to position. The phase of a given spin is the integral of its precession frequency from the time it was created to the time that is observed. If the applied gradient waveform is

$$\mathbf{G}(t) = G_x(t)\mathbf{i} + G_y(t)\mathbf{j} + G_z(t)\mathbf{k} \qquad (1.4)$$

the phase of a spin at $\mathbf{x}$ is

$$
\begin{aligned}
\phi(t) &= \int_0^t (-\gamma \mathbf{G}(s)) \cdot \mathbf{x}\, ds & (1.5)\\
&= \left(-\gamma \int_0^t \mathbf{G}(s) ds \right) \cdot \mathbf{x} & (1.6)\\
&= -2\pi\, \mathbf{k}(t) \cdot \mathbf{x}, & (1.7)
\end{aligned}
$$

where

$$\mathbf{k}(t) = \frac{\gamma}{2\pi} \int_0^t \mathbf{G}(s) ds. \qquad (1.8)$$
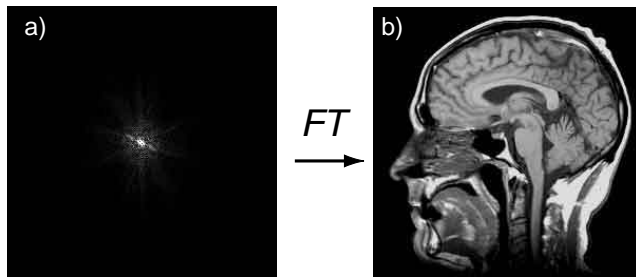
Figure 1.6: Sample MRI data, and the image reconstructed from this data.

Figure 1.7: A 2DFT, or spin-warp, pulse sequence and k-space coverage.

The negative sign is due to the negative precession direction of protons. The magnetization at time t is the original magnetization multiplied by the phase accrued during the free precession interval

$$M_{xy}(t, \mathbf{x}) = M_{xy}(\mathbf{x})e^{-i2\pi \mathbf{k}(t)\cdot\mathbf{x}}. \qquad (1.9)$$

where the time variable is suppressed for the initial magnetization.

The RF receive coil is spatially non-selective, and simply integrates over the entire volume

$$s(t) = \int_{\mathbf{X}} M_{xy}(\mathbf{x})e^{-i2\pi \mathbf{k}(t)\cdot\mathbf{x}}d\mathbf{x} \qquad (1.10)$$

where $\mathbf{X}$ ranges over the subject volume.

This expression has a familiar form. The factor $e^{-i2\pi \mathbf{k}(t)\cdot\mathbf{x}}$ is a Fourier kernal. By integrating over $\mathbf{x}$ we are taking the Fourier transform of the spatial distribution of the initial magnetization $M_{xy}(\mathbf{x})$. We will define the forward transform to have the minus sign in the exponent. At time t the signal we receive $s(t)$ is simply the value of the Fourier transform of $M_{xy}(\mathbf{x})$ sampled at the spatial frequency $\mathbf{k}(t)$. Acquiring an MRI image is performed by sampling the spatial frequency content of the image directly, and then performing an inverse Fourier transform to reconstruct the image. Figure 1.6 shows an example of the raw acquired spatial frequency data, and the image that it reconstructs to.
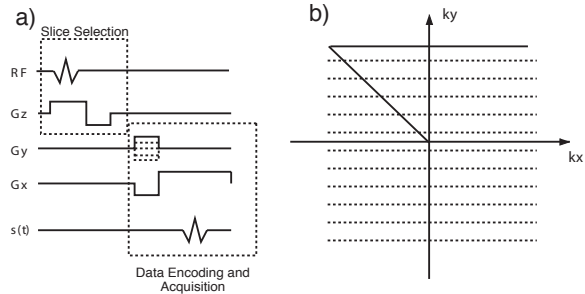
1.3 MRI Acquisition Methods

From the perspective of Eq. 1.10 it is clear that there are many different ways to acquire MRI data. The requirement is simply that enough of spatial frequency space, or k-space, be sampled to allow an image to be reconstructed.

1.3.1 2DFT, or Spin-Warp

By far the most common way to sample k-space is with a rectilinear raster scan. This is known as a 2DFT acquisition, because the 2DFT of the image is directly acquired. Image reconstruction is performed with a simple 2D FFT. This method is also known by the more colorful name "spin-warp".

MRI acquisition methods are most often described by pulse sequence diagrams, that show the timing and amplitudes of the application of the gradient fields on different axes, as well as the timing of the RF pulses. A pulse sequence for a 2DFT pulse sequence is shown in Fig. 1.7. Two basic elements of the pulse sequence are identified by dotted lines. The first is the slice-selective excitation that was described schematically in the previous section. This prepares the magnetization in a slice for imaging.

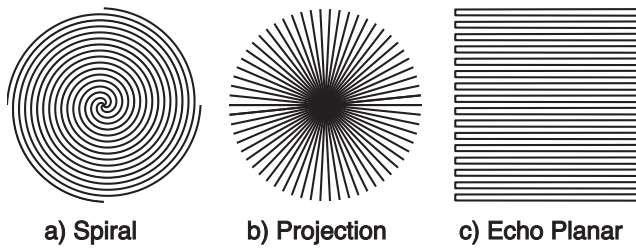The second element is the 2DFT acquisition gra-

Figure 1.8: Alternative k-space trajectories.

dients. The k-space position is the integral of the gradient waveforms. The 2DFT acquisition consists of two stages. First, gradient lobes move the k-space position to the beginning of one of the raster lines. A fixed area negative x gradient lobe, called a dephaser, moves the k_x position to the same initial value for each line. A variable area y gradient lobe, called the phase-encode, moves the k_y position to a specific line in k-space. Then a constant gradient is applied to the x gradient to scan along this line in k-space, while the raw MRI data is acquired. This is repeated typically 128 or 256 times, until enough data has been acquired to reconstruct an image. A 2D FFT is then applied to perform the reconstruction. The example shown in Fig. 1.6 was acquired and reconstructed in this way.

1.3.2   Other Alternatives

2DFT imaging has many advantages. It is insensitive to many hardware imperfections, and to variations in the main magnetic field. However, because it requires a large number of acquisitions, it is relatively slow. On a current high-performance 1.5 T whole body system, the minimum repetition time, T_R is on the order of 2.5 ms. To acquire 128 phase-encodes, or lines in k-space, takes 384 ms, which is not quite 3 images per second. This is inadequate for many high-speed imaging applications, such as real-time imaging of the beating heart.

There are many other alternatives methods for acquiring the k-space data for MRI images. Several important ones are shown in Fig. 1.8. Many others can be imagined. In a perfect world, where the gradient waveforms do exactly what they should, the subject is precisely on resonance, and the MR signal persists indefinitely, any of these would work well. In practice, none of the conditions hold, and the success of these different approaches depends critically on the effects of these imperfections, and whether these effects can be corrected in the reconstruction.

The spiral acquisition shown in Fig. 1.8a typically starts at the origin of k-space, and spirals outward. This can be done in a single acquisition, or in multiple rotated acquisitions, so as to cover k-space uniformly. The main advantages of spirals are very good flow properties, and flexibility in trading off readout duration and imaging speed. The main disadvantage is image blurring with changes in the resonant frequency. Reconstruction methods that correct for this blurring will be a major subject in this class.

The projection acquisition methods shown in Fig. 1.8b was actually one of the earliest methods used for MRI, due to the previous success of CT. It was largely abandoned with the advent of spin-warp, but has been revived for several specific applications. One is 3D angiography, where a 3D volume is reconstructed, and then reprojected. The imaging characteristics of projection acquisitions allows tremendous undersampling while maintaining resolution for this case of sparse, high contrast objects. The main disadvantage of projection acquisitions is off-resonance blurring, as for spirals. Many of the spiral reconstruction methods can be adapted to projection acquisitions.

The most common high-speed imaging method is echo-planar, or EPI, shown in Fig. 1.8c. This can be considered as an extension of spin-warp, where multiple lines in k-space are acquired after a single excitation. This can be done in a single shot, or

in multiple interleaved acquisitions. EPI has the advantage of allowing for a 2DFT reconstruction, and that off-resonance produces geometric distortion primarily, and no image blurring. EPI has the disadvantage of producing image ghosts for almost any hardware imperfection or subject motion. Hence, EPI reconstruction requires great attention to detail to make high fidelity images, as will be described.

1.3.3   Sampling, FOV, and Resolution

In this course we are often going to need to be able to compute specific numbers for sample spacing, field of view, and image resolution. The relationship between these parameters was described in [1]. The basic relationships are summarized here.

There are four interrelated parameters in each dimension. For the x dimension the first is the field of view FOV_x. This is the dimensions of the image, and is typically measured in centimeters. The next is the image resolutions Δx. Ideally this is the minimum distance that two point sources can be resolved. It is typically cited in millimeters. The third is the maximum radius in k-space that was collected, $k_{x,max}$, measured in cycles/cm. The final parameter is the density of sampling in k-space, Δk_x. The FOV and $k_{x,max}$ are illustrated in Fig. 1.9.

The relationship between these parameters is simple. In each case, the extent in one domain multiplied by the resolution in the other domain is unity. Hence

$$FOV_x \Delta k_x = 1 \qquad (1.11)$$

and

$$2k_{x,max} \Delta x = 1 \qquad (1.12)$$

since the extent in k-space goes from $-k_{x,max}$ to $+k_{x,max}$. In addition, if N_x is the number of samples in either domain, then

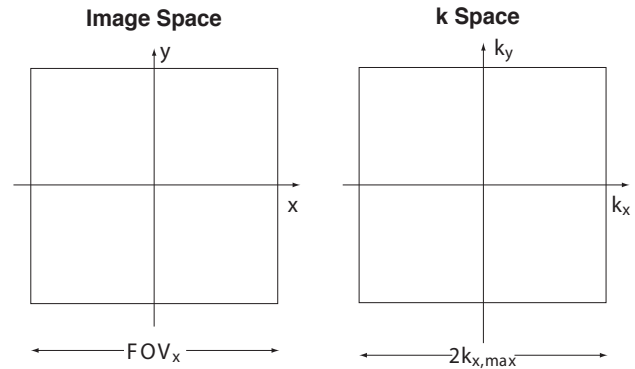$$FOV_x = N_x \Delta x \qquad (1.13)$$

Figure 1.9: Definitions of FOV in image space, and $2k_{x,max}$ in k-space.

and

$$2k_{x,max} = N_x \Delta k_x. \qquad (1.14)$$

These equations make intuitive sense if you consider the effect of phase encoding steps for the case of the y dimension. Each step adds one cycle of phase shift across the FOV. If one phase encode is zero, then the next, at $+\Delta k_y$ produces one cycle over the FOV, so $\Delta k_y = 1/FOV$, and $FOV \Delta k_y = 1$.

1.4   Physical Realities

In the derivation of the signal equation we neglected a number of factors that will be important during this course. One important factor is that the resonant frequency of the subject varies with space. Another is that the magnetization decays while data is being acquired. Finally, the gradient system interacts with other parts of the scanner, and this contributes phase errors, and inaccuracies in k-space trajectories.

1.4.1 Variations in Resonant Frequency

Variations in resonant frequency come from two sources. One is that different chemical species have different resonant frequencies. In imaging we are mostly concerned with water. However, the body also contains lipids which have several resonant frequencies. The main component of concern is 3.4 ppm away from the water line, or about 217 Hz away from the water line at 1.5T. Since data acquisition window can be tens of milliseconds in duration, the lipid-water shift can result in many cycles at the lipid frequency when tuned to the water frequency. This causes a displacement in spin-warp and EPI acquisitions, and blurring with spiral and projection acquisitions.

The other source of resonant frequency variation is due to the magnetic susceptibility of tissue, and the geometry of the subject. Tissue has a magnetic susceptibility of about 10 ppm with respect to air, or a vacuum. According to Maxwell's equations, magnetic flux is conserved at a boundary perpendicular to magnetic field lines, so that there is a 10 ppm discontinuity in field, and hence resonant frequency at such boundaries. Other boundary orientations and geometries produce lesser shifts. The result is that a body itself produces a variation in resonant frequency of several ppm, with the resonant frequency denoted by $\omega(\mathbf{x})$.

1.4.2 Relaxation

Magnetization decay during the acquisition is due the loss of coherence of the spins. This can be due to the irreversible exchange of energy between spins, which is known as T_2 decay, or spin-spin relaxation. It can also be due to a reversible loss of coherence, from variations of precession frequency over a voxel. This is known as T_2^* decay. The formation of spin-echoes suppresses T_2^*.

If the off-resonance reception and the T_2 signal decay are included in Eq. 1.9, we get

$$M_{xy}(t, \mathbf{x}) = M_{xy}(\mathbf{x})e^{-i2\pi\mathbf{k}(t)\cdot\mathbf{x}}e^{(-\frac{1}{T_2}-i\omega(\mathbf{x}))t}.$$
(1.15)

Integrating over space, as before, the received signal becomes

$$s(t) = \int_{\mathbf{X}} M_{xy}(\mathbf{x})e^{(-\frac{1}{T_2}-i\omega(\mathbf{x}))t}e^{-i2\pi\mathbf{k}(t)\cdot\mathbf{x}}d\mathbf{x}.$$
(1.16)

The received signal is samples of a Fourier transform. The difference is that the Fourier transform corresponds to a magnetization $M_{xy}(\mathbf{x})$ that has been weighted by $e^{(-\frac{1}{T_2}-i\omega(\mathbf{x}))t}$.

1.4.3 Eddy Currents

Another important source of errors in MR data acquisition is due to eddy currents induced by the gradient coil. The gradient coil is designed to produce linear variations in the z component of the magnetic field *inside* the coil. However, it also produces fields *outside* the coil, and these can interact with other elements of the scanner, such as the aluminum bore tube. The changing field from the gradient coil induces eddy currents in the bore tube. These eddy currents produce an additional field inside the gradient coil that tends to oppose and lag the desired gradient field, corrupting the MR measurements.

Two methods are commonly used to minimize the effects of eddy currents. One is to add an active shield to the gradient coil. This is essentially a larger coil that enclosed the primary gradient coil, that cancels out the external fields that would otherwise interact with the bore tube. The other approach is to pre-emphasize the gradient waveform, so that the combination of the fields from the gradient coil and the eddy currents produce the desired waveform. These both work well, and eliminate the vast majority of the errors from eddy currents. However, there is frequently enough residual

error to require additional compensation in pulse sequence design, or correction in reconstruction.

The magnetic fields produced by the eddy currents cause an additional frequency modulation of the received signal. This modulation is a function of the applied gradient, and is both time varying and spatially varying. We will model this frequency as

$$\begin{aligned} \omega_e(\mathbf{x}, t) &= \gamma \mathbf{G}(t) * \mathbf{h}_0(t) \cdot \mathbf{1} + \\ &\qquad \gamma \mathbf{G}(t) * \mathbf{h}_1(t) \cdot \mathbf{x} \quad (1.17) \\ &= \omega_{e,0}(t) + \gamma \mathbf{G}_e(t) \cdot \mathbf{x} \qquad (1.18) \end{aligned}$$

where the dot product with $\mathbf{1}$ simply sums the contributions from each axis. This model consists of two terms. The first term (the "B_0" term) is constant in space, and has a time dependence that is given by a convolution of the gradient waveform with an impulse response. The second term (the gradient term) is linear in space, and has a time dependence that is the convolution of the gradient waveform with a second impulse response.

There are higher order spatial dependence terms that we are neglecting. Also, the assumption of a convolution temporal dependence is not always reasonable. For example, if the eddy currents occur in the highly saturated iron core of a resistive magnet, the response can be very non-linear. However, for a high-field superconducting system, this approximation accounts for most of the eddy-current effects.

The real reason for using this model is that the two terms correspond to physical quantities we control. The first is the center frequency of the system, and the second is the gradient waveform. On a high-performance system, each of the two impulse responses is measured experimentally as part of system calibration. The first term is corrected by computing the modeled B_0 term, and using this as the system center frequency. As long as the system and the magnetization accurately track each other, it doesn't matter that the frequency is drifting.

The second term is corrected by applying a pre-emphasis filter to the gradient waveform. The combination of the field from the primary gradient and shield, and the fields due to eddy currents produces the desired, ideal, gradient field. The use of gradient pre-emphasis filters has long been a part of all MR systems.

In practice, even after all of these corrections, there are still significant eddy-current induced frequency shifts that effect the acquired data. There are several reasons for this. One is that it is difficult to measure and model the very short time-constant terms. Another is that other conducting elements, like RF coils, can contribute, and these vary from acquisition to acquisition as the RF coils and their placement change.

For our purposes, we have to keep in mind that eddy currents will corrupt our measurements. The eddy currents produce a time varying frequency shift. The received signal will be phase modulated by the integral of this frequency shift over time

$$\begin{aligned} \int_0^t \omega_e(\tau)\, d\tau &= \int_0^t \omega_{e,0}(\tau)\, d\tau + \\ &\qquad \int_0^t \gamma \mathbf{G_e}(\tau) \cdot \mathbf{x}\, d\tau (1.19) \\ &= \theta_e(t) + 2\pi \mathbf{k}_e(t) \cdot \mathbf{x} \quad (1.20) \end{aligned}$$

The signal equation neglecting T_2 and off-resonance, is then

$$\begin{aligned} s(t) &= \int_{\mathbf{X}} M_{xy}(\mathbf{x}) e^{(-i\theta_e(t) - i2\pi \mathbf{k}_e(t) \cdot \mathbf{x})} e^{-i2\pi \mathbf{k}(t) \cdot \mathbf{x}} d\mathbf{x} \\ &\qquad\qquad\qquad\qquad\qquad\qquad (1.21) \\ &= \int_{\mathbf{X}} M_{xy}(\mathbf{x}) e^{-i\theta_e(t)} e^{-i2\pi(\mathbf{k}(t) + \mathbf{k}_e(t)) \cdot \mathbf{x}} d\mathbf{x}, \\ &\qquad\qquad\qquad\qquad\qquad\qquad (1.22) \end{aligned}$$

where the minus sign in the exponent comes from the negative sense of the precession of protons. We see we should expect two types of errors. One is a spatially isotropic phase modulation that depends on the gradient waveform. The second is an error in the k-space trajectory, that also depends on the gradient waveform.

1.4.4 Implications for Pulse Sequence Design

There are many different methods that have proposed for acquiring MR data. The success of a particular method depends critically on how each of the factors described above effect the reconstructed images. Ideally, imaging methods should be designed to be immune to these errors. Spinwarp is an excellent example. Off-resonance, T_2, and B_0 and gradient eddy current terms produce miminal or benign artifacts in spin warp. The cost for this is long scan times. Fast imaging methods are based on acquisitions that are sensitive to these errors, but in ways that can be characterized and corrected in reconstruction. For example, eddy currents produce ghosts in EPI. However, these can be estimated and corrected as part of the reconstruction. Off-resonance causes blurring in spirals, but again this can be significantly corrected in reconstruction.

1.5 References

1. *Magnetic Resonance Imaging*, Dwight G. Nishimura, MRSRL Press

2. *Magnetic Resonance Imaging: Physical Principles and Sequence Design*, E. Mark Haacke, Robert W. Brown, Michael R. Thompson, and Ramesh Venkatesan, Wiley, 1999.

3. *Principles of Magnetic Resonance Imaging: A Signal Processing Approach*, Zhi-Pei Liang and Paul C. Lauterbur, IEEE Press, 2000.

4. *Foundations of Medical Imaging*, Zang-Hee Cho, Joie P. Jones, and Manbir Singh, Wiley, 1993.

5. *Medical Imaging Systems*, Albert Macovski, Prentis-Hall, 1983.

6. *Principles of Computed Tomography*, Avinash C. Kak and Malcolm Slaney, IEEE Press, 1988 (now reprinted by SIAM).

7. Paul C. Lauterbur. Nature 242:190, 1973